



**HAL**  
open science

## Role of goethite during air-oxidation of PAH-contaminated soils

Coralie Biache, Olivier Kouadio, Khalil Hanna, Catherine Lorgeoux, Pierre  
Faure

► **To cite this version:**

Coralie Biache, Olivier Kouadio, Khalil Hanna, Catherine Lorgeoux, Pierre Faure. Role of goethite during air-oxidation of PAH-contaminated soils. *Chemosphere*, 2014, 117, pp.823-829. 10.1016/j.chemosphere.2014.11.004 . hal-01101620

**HAL Id: hal-01101620**

**<https://univ-rennes.hal.science/hal-01101620>**

Submitted on 13 Jan 2015

**HAL** is a multi-disciplinary open access archive for the deposit and dissemination of scientific research documents, whether they are published or not. The documents may come from teaching and research institutions in France or abroad, or from public or private research centers.

L'archive ouverte pluridisciplinaire **HAL**, est destinée au dépôt et à la diffusion de documents scientifiques de niveau recherche, publiés ou non, émanant des établissements d'enseignement et de recherche français ou étrangers, des laboratoires publics ou privés.

# Role of goethite during air-oxidation of PAH-contaminated soils

Coralie Biache<sup>1,2,\*</sup>, Olivier Kouadio<sup>1,2</sup>, Khalil Hanna<sup>3</sup>, Catherine Lorgeoux<sup>4,5</sup>, Pierre Faure<sup>1,2</sup>

<sup>1</sup> Université de Lorraine, LIEC, UMR7360, Vandœuvre-lès-Nancy, F-54506, France

<sup>2</sup> CNRS, LIEC, UMR7360, Vandœuvre-lès-Nancy, F-54506, France

<sup>3</sup> École Nationale Supérieure de Chimie de Rennes, UMR CNRS 6226, 11 Allée de Beaulieu, F-35708 Rennes Cedex 7, France.

<sup>4</sup> Université de Lorraine, GeoRessources, UMR7359, Vandœuvre-lès-Nancy, F-54506, France

<sup>5</sup> CNRS, GeoRessources, UMR7359, Vandœuvre-lès-Nancy, F-54506, France

## \* Corresponding author

Address: LIEC, Faculté des Sciences et Techniques

Boulevard des Aiguillettes

B.P. 70239

54506 Vandoeuvre-lès-Nancy Cedex

France

E-mail: coralie.biache@yahoo.fr (C. Biache)

Phone: (+33) 3 83 68 47 40

24 **Abstract**

25 The impact of goethite on air-oxidation of PAH-contaminated soils was studied through two  
26 sets of experiments. (i) Soil extractable organic matter (EOM) and (ii) whole coking plant  
27 soils were oxidized at 60 and 100 °C for 160 days, with/without goethite. Organic matter  
28 (OM) mineralization was monitored via CO<sub>2</sub> production and polycyclic aromatic compounds  
29 (PACs) oxidation was investigated by GC-MS analyses. The decrease in EOM and PAH  
30 contents, and the oxygenated-PAC production observed during EOM oxidation, were  
31 enhanced by the presence of goethite. PACs were likely transformed at the goethite surface  
32 through electron transfer process. Mass carbon balance revealed a transfer from EOM to the  
33 insoluble organic fraction indicating condensation/polymerization of organics. Soil oxidation  
34 induced a decrease in EOM, PAH but also in oxygenated-PAC contents, underscoring  
35 different oxidation or polymerization behavior in soil. The goethite addition had a lesser  
36 impact suggesting that indigenous minerals played an important role in PAC oxidation.

37 **Keywords:** contaminated soil; polycyclic aromatic compound (PAC); oxygenated-PAC;  
38 goethite; oxidation

39

## 40 1. Introduction

41

42 Iron oxides are the most abundant metallic oxides in soils (Schwertmann and Taylor, 1989),  
43 they are present in most soils and encompass oxides, oxyhydroxides and hydrated oxides. Fe-  
44 minerals are known to play an active part in the organic contamination fate as they represent  
45 strong sorption surfaces for pollutants and they catalyze many important redox  
46 transformations (Borch et al., 2009). During the past decades their ability to participate in  
47 such redox reactions was involved in remediation strategies for organic contamination. For  
48 instance Fe-minerals are associated with H<sub>2</sub>O<sub>2</sub> to produce hydroxyl radicals that can degrade  
49 organic compounds in Fenton-like reactions. Soil iron minerals i.e. magnetite, hematite,  
50 goethite, and ferrihydrite, are all able to catalyze H<sub>2</sub>O<sub>2</sub> (Yap et al., 2011).

51 Fenton-like reaction has been investigated for the remediation of water and soil contaminated  
52 with halogenated solvent, pesticides and petroleum hydrocarbons (Watts and Stanton, 1999;  
53 Usman et al., 2013). Fenton-like reaction shows also a great potential for polycyclic aromatic  
54 hydrocarbon (PAH, compounds constituted of two, or more, fused benzene rings) degradation  
55 in contaminated soils (Nam et al., 2001; Usman et al., 2012). The catalytic role of iron oxides  
56 for Fenton-like reaction is extensively studied for chemical remediation purpose. However  
57 such treatments are not automatically applied to contaminated soils and little is known about  
58 the involvement of iron oxide in processes occurring during natural attenuation of  
59 contaminated soils, especially abiotic oxidation. Some authors studied iron oxide-mediated  
60 oxidative transformations of organic compounds (Zhang and Huang, 2007; Lin et al., 2012)  
61 but the experiments were designed with solids suspended in aqueous solution which is not  
62 representative of real soil conditions. Wang et al. (2009) studied pyrene degradation on iron  
63 oxide under UV radiation and evidenced photocatalytic effect of several iron oxide. In real

64 soils UV light affects only the surface layers since its intensity decays rapidly in the solid  
65 phase. Abiotic oxidation still occurs in deeper layer but so far this process was scarcely  
66 investigated, probably due to the difficulty to study this process independently to others. This  
67 difficulty can be bypassed using experimental simulation. Indeed low-temperature oxidations  
68 (60-130 °C) are proven to successfully mimic long-term abiotic oxidation of fossil organic  
69 matter (OM) (Faure et al., 1999; Elie et al., 2000; Blanchart et al., 2012). Such experiments  
70 were extensively used in the 1980s to study coal weathering and its impact on coal heating  
71 properties (Gethner, 1987; Calemma et al., 1988; Jakab et al., 1988). More recently, low-  
72 temperature oxidations of PAH-contaminated matrices showed that minerals (e.g. clay  
73 minerals and calcite) play an important role on the contamination fate (Ghislain et al., 2010;  
74 Biache et al., 2011; Biache et al., 2014). Indeed, oxidation causes a production of oxygenated-  
75 polycyclic aromatic compounds (O-PACs: PAH with oxygenated moieties e.g. alcohol,  
76 ketone, aldehyde groups) and formation of an insoluble carbonaceous residue, supposedly  
77 through oxidative polymerization, leading to the contamination stabilization. PAH-  
78 contaminated soils often contain high proportion of iron oxide and other metal oxides (Biache  
79 et al., 2014), however their influence on PAC oxidation has never been investigated in such  
80 context.

81 Therefore, this study reported a first investigation on the role of iron oxide (goethite) on  
82 PAC fate (including PAHs and O-PACs) during abiotic air-oxidation of contaminated soils.  
83 Its aim was to determine which mechanisms were involved during this major process involved  
84 in natural attenuation. Goethite ( $\alpha$ -FeOOH) was selected because it is one of the most  
85 thermodynamically stable and the most abundant iron (oxy)(hydr)oxide in natural  
86 environments (Schwertmann and Cornell, 2007).  
87 Two sets of experiments were performed. The first one was conducted on extractable organic  
88 matter (EOM) previously isolated from PAC-contaminated soils. Afterwards, EOM was

89 mixed with goethite or silica sand; the latter was used as inert support since its reactivity  
90 towards organic compounds is limited (Ghislain et al. 2010). The second experiment was  
91 performed directly on soils, raw or supplemented with goethite. These two sets allowed  
92 investigating two levels of increasing complexity by studying the influence of an iron oxide  
93 on the soil EOM, which could give more precise information on the involved mechanisms,  
94 and on the whole soil including indigenous minerals, which is more complex but also more  
95 realistic. Oxidations were performed at 60 and 100 °C, the latter allowing more advanced  
96 oxidation and the first one representing an intermediate between 100 °C and field  
97 temperatures.

98

## 99 **2. Materials and Methods**

### 100 2.1. Samples

101 Soils were sampled at two former coking plant sites (Homécourt and Neuves-Maisons,  
102 France), then freeze-dried, sieved (2 mm) and crushed (500 µm). EOM was recovered by  
103 extracting parts of the soils in Soxhlet apparatus (CHCl<sub>3</sub>, 24 h), it contains PACs and other  
104 organics of various size, from macromolecules (asphaltenes) to mono-aromatic units. Neuves-  
105 Maisons and Homécourt EOMs were concentrated at 1.4 and 2.4 mg/mL, respectively. Soils  
106 were also used directly or mixed with goethite.

107

### 108 2.2. Minerals

109 The silica sand was Fontainebleau sand (180-500 µm, Carlo Erba) used as a non-reactive  
110 reference in the EOM experiment.

111 Goethite ( $\alpha$ -FeOOH) was synthesized according to Schwertmann and Cornell (2007).  
112 Briefly, sample was prepared by air-oxidation of a hydrolyzed FeSO<sub>4</sub> solution according to  
113 Prélot et al. (2003) (cf. supporting information).

114 Minerals were washed with dichloromethane prior experiments to prevent organic  
115 contamination.

116

### 117 2.3. Oxidation experiment

118 EOMs and soils were mixed with minerals according to the following proportions: silica  
119 sand (2 g) and goethite (0.5 g) mixed with Homécourt (47.1 mg) and Neuves-Maisons (48.7  
120 mg) EOMs, Homécourt (2.5 g) and Neuves-Maisons (5 g) soils taken alone or mixed with  
121 goethite (0.5 g) (Table S1). Soils and minerals were placed in 100 mL glass bottles equipped  
122 with open caps and PTFE/silicone septa. EOM aliquots were added to the minerals to reach  
123 the mineral/EOM proportions specified in Table S1. Bottles were left open in a ventilated  
124 hood until complete evaporation of the solvent.

125 Two sample sets were prepared and placed in ovens at 60 and 100 °C. CO<sub>2</sub> released in the  
126 bottles was measured weekly by an infrared absorbance measurement ( $\lambda = 2325.6 \text{ cm}^{-1}$ ) with  
127 an infrared Binos analyzer. The measured CO<sub>2</sub> was normalized to the initial sample total  
128 organic carbon (TOC) content. After each measurement bottles were opened to renew the  
129 atmosphere and the septa were replaced. After 160 days, samples were removed from the  
130 ovens and, after CO<sub>2</sub> measurements, were stored at -18 °C prior analyses.

131

### 132 2.4. Extraction

133 Samples were transferred to 250 mL boiling flasks and chloroform (100 mL) was added to  
134 each flask. The mixtures were heated at 60 °C and stirred for 45 min before being filtered on  
135 GF/F Whatman glass-fiber filters. The filtrates were concentrated under a gentle nitrogen flow  
136 and volumes were adjusted to 20 mL. For each sample, an EOM fraction (3 mL) was  
137 transferred to a pre-weighed bottle and the EOM content was determined after solvent  
138 evaporation.

139

## 140 2.5. PAC quantification

141 An internal PAH standard mix of [<sup>2</sup>H<sub>8</sub>]naphthalene, [<sup>2</sup>H<sub>10</sub>]acenaphthene,  
142 [<sup>2</sup>H<sub>10</sub>]phenanthrene, [<sup>2</sup>H<sub>12</sub>]chrysene, [<sup>2</sup>H<sub>12</sub>]perylene (25 µL at 16 µg/mL, Cluzeau) was added  
143 to the EOM (75 µL) before being injected in a gas chromatograph coupled with a mass  
144 spectrometer (GC-MS). The GC-MS was previously internally calibrated with the internal  
145 standards listed above for 16 PAHs plus 4 O-PACs (Table 1) at 6 concentrations (0.5, 1, 2, 4,  
146 6 and 8 µg/mL). The GC was a Shimadzu GC-2010 Plus, equipped with a silica-glass  
147 capillary column DB-5MS (60 m × 0.25 mm i.d. × 0.1 µm film thickness) coupled with a  
148 QP2010-Ultra (Shimadzu) MS in fullscan mode with a transfer line heated at 300 °C. The  
149 oven temperature program was as follow: 70 °C for 2 min, from 70 to 130 °C at 15 °C/min,  
150 then from 130 to 315 °C at 3 °C/min and then a 15-min hold at 315 °C. Helium was used as  
151 carrier gas in constant flow mode (1.4 mL/min).

152

## 153 2.6. TOC content

154 TOC contents were determined in soils and EOM/mineral mixtures with a total carbon  
155 analyser TOC-V CSH (Shimadzu) associated with a solid sample module SSM-5000A  
156 (Shimadzu).

157

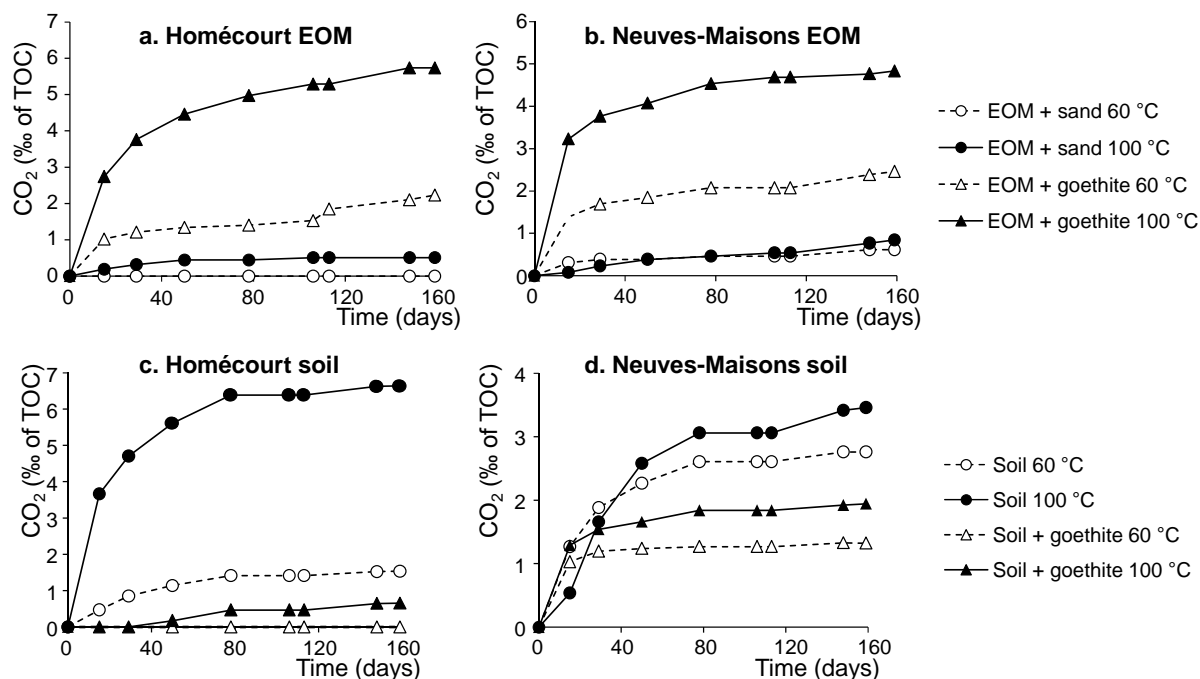
## 158 3. Results

### 159 3.1. EOM/minerals mixture

#### 160 3.1.1. CO<sub>2</sub> production

161 For both samples, CO<sub>2</sub> production of the EOM/mineral mixture followed the same trend  
162 (Figure 1a,b). The maximum production was observed for the EOM/goethite mixtures

163 oxidized at 100 °C and reached about 6 and 5‰ of TOC for Homécourt and Neuves-Maisons,  
 164 respectively. It was followed by the CO<sub>2</sub> produced by the EOM/goethite mixture during the  
 165 60 °C oxidation. Smaller amount of CO<sub>2</sub> were observed for the EOM/sand mixture  
 166 oxidations.

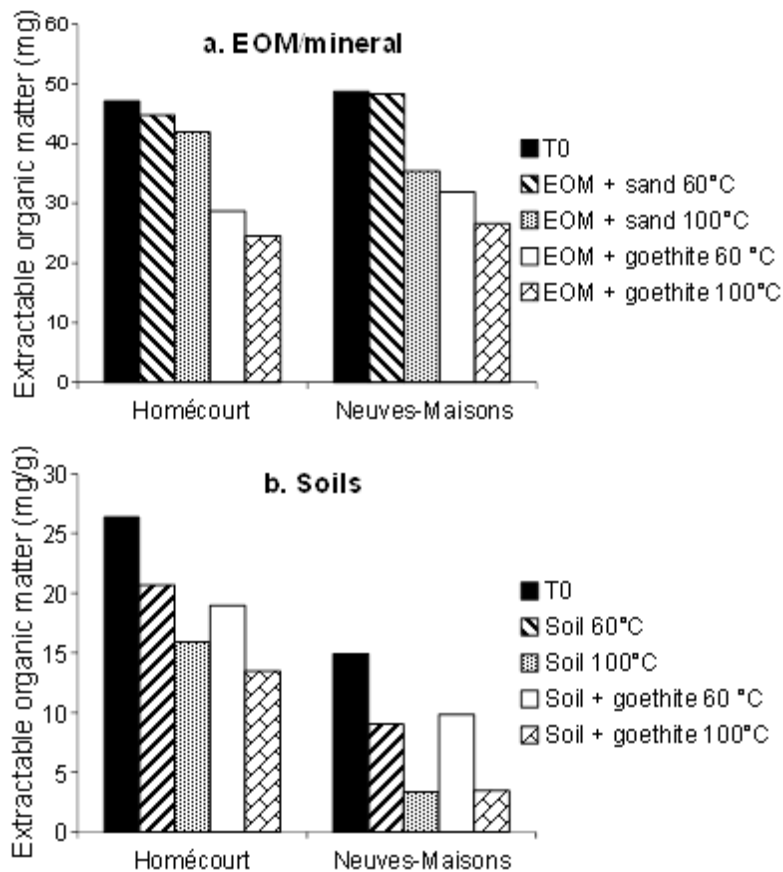


167  
 168 *Figure 1: CO<sub>2</sub> production during the 60 and 100 °C oxidation experiments of the extractable organic*  
 169 *matter (EOM) from (a.) Homécourt and (b.) Neuves-Maisons samples, mixed with silica sand and*  
 170 *goethite, and (c.) Homécourt and (d.) Neuves-Maisons soils and soils mixed with goethite.*

171

### 172 3.1.2. EOM contents

173 Overall, oxidations induced a decrease in the EOM content of the EOM/mineral mixtures  
 174 (Figure 2a). It was limited for the EOM/sand mixtures oxidized at 60 °C and was more  
 175 important for the same mixture oxidized at 100 °C but clearly lower than the EOM/goethite  
 176 mixtures. The decrease was similar for both Homécourt and Neuves-Maisons samples at 100  
 177 °C and went from 47.1 to 24.5 mg and from 48.7 to 26.6 mg, respectively.



178

179 *Figure 2: Extractable organic matter (EOM) contents after the 60 and the 100 °C oxidation*  
 180 *experiment of (a.) Homécourt and Neuves-Maisons EOM/mineral mixtures, and (b.) Homécourt and*  
 181 *Neuves-Maisons soil and soil/goethite mixtures.*

182

### 183 3.1.3. PAH contents

184 Overall, EOM/mineral mixture oxidations induced a decrease in PAH concentrations. For  
 185 Homécourt EOM/sand mixture it was limited to 5% after the 60 °C experiment (Table 1). It  
 186 was more important at 100 °C (49%), mostly because of the loss of low molecular weight  
 187 (LMW) compounds compared to high molecular weight (HMW), as shown by the  
 188 LMW/HMW ratio which went from 3.1 to 1 (Table 1). The 60 and 100 °C experiments  
 189 induced a decrease in PAH content of 27% and 59% for Homécourt EOM/goethite mixture,  
 190 respectively. It affected again mainly LMW PAHs, especially the 2- and 3-ring PAHs (Table  
 191 1, Figure S3).

192 Contrary to the Homécourt EOM/sand mixture, PAHs decreased notably (40%; Table 1) after  
193 the 60 °C oxidation of the Neuves-Maisons EOM/sand mixture. This decrease affected both  
194 LMW and HMW compounds (Table 1, Figure S4). It was confirmed by the LMW/HMW ratio  
195 which was barely modified (Table 1). At 100 °C, the PAH decrease was more important and  
196 reached 61%. The LMW PAH, especially the 2- and 3-ring compounds were more affected  
197 (Table 1, Figure S4). Neuves-Maisons EOM/goethite mixture oxidations induced also a  
198 decrease in the PAH contents. It was relatively close whatever the temperature (63% at 60 °C  
199 and 66% at 100 °C; Table 1)

200

#### 201 *3.1.4. O-PAC contents*

202 Overall, oxidations induced an increase in the O-PAC contents (Table 1). For Homécourt  
203 EOM, it was more important at 60 °C than at 100 °C. It was also higher when the EOM was  
204 mixed with goethite than when mixed with sand (Table 1). The O-PAC production concerned  
205 mostly 9-fluorenone and anthracene-9,10-dione (Table 1, Figure S5). The increase in O-PAC  
206 concentrations in Neuves-Maisons EOM/mineral mixtures was higher at 100 °C than at 60 °C  
207 (Table 1). The maximum O-PAC production reached 203% when Neuves-Maisons EOM was  
208 mixed with goethite and oxidized at 100 °C (Table 1). This increase affected mostly  
209 benzo[*de*]anthracene-7-one and benz[*a*]anthracene-7,12-dione (Table 1, Figure S6).

210 .

Table 1: PAH and O-PAC contents (in  $\mu\text{g/g}$ ) of the initial and oxidized (60 °C and 100 °C) extractable organic matter (EOM)/mineral mixture

$\mu\text{g/g}$	Homécourt					Neuves-Maisons				
	Initial	EOM/sand 60°C	EOM/sand 100°C	EOM/goet. 60°C	EOM/goet. 100°C	Initial	EOM/sand 60°C	EOM/sand 100°C C	EOM/goet. 60°C	EOM/goet. 100°C
Naphthalene	17	2.0	n.d.	n.d.	n.d.	240	7.6	n.d.	n.d.	n.d.
Acenaphthylene	290	250	160	160	93	170	99	26	49	24
Acenaphthene	600	410	n.d.	61	n.d.	150	71	n.d.	n.d.	n.d.
Fluorene	410	260	20	39	22	120	65	2.5	7.0	1.3
Phenanthrene	750	760	150	720	320	390	270	21.1	130	34
Anthracene	220	260	120	150	67	170	150	37	39	31
Fluoranthene	400	550	300	560	260	550	440	220	320	220
Pyrene	290	320	240	310	200	450	290	180	200	150
Benz[ <i>a</i> ]anthracene	190	150	140	140	46	480	290	220	160	160
Chrysene	150	180	190	180	170	500	330	310	240	310
Benzo[ <i>b</i> ]fluoranthene	210	180	260	170	190	650	360	350	300	340
Benzo[ <i>k</i> ]fluoranthene	61	57	71	54	56	320	210	200	140	170
Benz[ <i>a</i> ]pyrene	140	130	39	94	4.9	500	290	110	150	0.6
Indeno[ <i>cd</i> ]pyrene	110	85	100	83	74	490	260	260	190	230
Dibenz[ <i>a,h</i> ]anthracene	34	63	69	68	44	170	81	110	58	92
Benzo[ <i>ghi</i> ]perylene	84	120	140	110	89	370	210	200	160	190
Sum of PAHs	3956	3777	1999	2899	1636	5720	3424	2247	2143	1953
PAH decrease (%)		5	49	27	59		40	61	63	66
LMW/HMW <sup>a</sup>	3.1	2.9	1.0	2.2	1.4	0.6	0.7	0.3	0.5	0.3
9-Fluorenone	530	780	680	1500	1200	160	180	48	180	130
Anthracene-9,10-dione	140	240	190	420	450	110	110	47	120	97
Benzo[ <i>de</i> ]anthracene-7-one	5.7	78	n.d.	82	n.d.	130	350	530	240	550
Benzo[ <i>a</i> ]anthracene-7,12-dione	n.d.	n.d.	120	71	n.d.	64	130	430	150	630
Sum of O-PACs	676	1098	990	2073	1650	464	770	1055	690	1407
O-PAC production (%)		62	46	207	144		66	127	52	203
%O-PAC (/total PAC)	15	23	33	42	50	8	18	32	24	42

212 <sup>a</sup>LMW/HMW = ratio of sum of naphthalene to pyrene relative to sum of benzo[*a*]anthracene to benzo[*ghi*]perylene

## 213 3.2. Soils and soil/goethite mixtures

### 214 3.2.1. CO<sub>2</sub> production

215 For Homécourt soil, the CO<sub>2</sub> production was higher when the raw soil was oxidized at 100 °C  
216 and reached 7‰ of the TOC at the end of the experiment (Figure 1c). The CO<sub>2</sub> production  
217 was much lower at 60 °C and reached less than 2‰ of the TOC. It was followed by the  
218 Homécourt soil/goethite mixture oxidized at 100 °C whereas the same mixture produced  
219 nearly no CO<sub>2</sub> at 60 °C (Figure 1c).

220 Similar pattern was observed for the Neuves-Maisons soil with a maximum CO<sub>2</sub> production  
221 for the raw soil oxidized at 100 °C which reached about 4‰ of the TOC. However the  
222 differences between the modalities were less pronounced and the minimum CO<sub>2</sub> production  
223 observed for the Neuves-Maisons/goethite mixture oxidized at 60 °C reached 1.3‰ of the  
224 TOC (Figure 1d).

225 It should be noted that a part of the generated gas could result from CO<sub>2</sub> desorption from soil  
226 solid surfaces (e.g. minerals, OM) over the soil thermal treatments, but this process may be  
227 insignificant under our experimental conditions (Sumner, 2000).

### 228 3.2.2. EOM contents

229 Soil oxidations led to a decrease in the EOM contents (Figure 2b). For both soils and  
230 soil/goethite mixtures, it was more important at 100 °C than at 60 °C. This decrease was  
231 enhanced by the presence of goethite in the case of Homécourt samples for which the EOM  
232 went from 26.4 to 19.0 and to 13.5 mg/g of soil after the 60 and the 100°C experiments,  
233 respectively. Surprisingly, no difference was observed with goethite addition to the Neuves-  
234 Maisons soil (Figure 2b).

### 235 3.2.3. PAH contents

236 Oxidations induced a strong decrease in the PAH concentrations for both soils. It was more  
237 important at 100 than at 60 °C and was maximum when goethite was added to the soil (92%  
238 of decrease for both samples; Table 2). For both samples, the 60 °C experiments affected  
239 slightly more HMW than LMW compounds, as shown by the increasing LMW/HMW ratios  
240 (Table 2). On the contrary, the 100 °C experiment induced a decrease in this ratio, indicating  
241 a preferential loss of the LMW PAHs (Table 2, Figures S7 and S8).

#### 242 3.2.4. *O-PAC contents*

243 Overall, the soil and soil/goethite mixture oxidations induced a decrease in the O-PAC  
244 contents. For the raw Homécourt soils, it was limited to 3% after the 100 °C experiment and  
245 reached 12% after the 60 °C oxidation. This decrease was higher when Homécourt soil was  
246 mixed with goethite and attained 18% and 41% after the 60 and the 100 °C experiments,  
247 respectively (Table 2, Figure S9).

248 The abatement rates were higher for the Neuves-Maisons soil with 54% and 60% after the 60  
249 and the 100 °C experiment on the raw soil, respectively. Goethite supplementation also  
250 enhanced this decrease but the proportion of O-PAC abatement was similar for both  
251 temperatures (71%; Table 2, Figure S10).

Table 2: PAH and O-PAC contents (in µg/g) of the initial and oxidized (60 °C and 100 °C) soils and soil/mineral mixtures

µg/g	Homécourt					Neuves-Maisons				
	Initial	Soil 60°C	Soil 100°C	Soil/goet. 60°C	Soil/goet. 100°C	Initial	Soil 60°C	Soil 100°C C	Soil/goet. 60°C	Soil/goet. 100°C
Naphthalene	9.4	4.5	0.3	3.6	n.d.	74	26	3.6	12	n.d.
Acenaphthylene	160	65	48	57	40	52	15	4.0	13	4.0
Acenaphthene	340	18	n.d.	13	n.d.	46	2.0	n.d.	1.6	n.d.
Fluorene	230	26	13	22	9.1	36	2.4	0.3	1.9	0.2
Phenanthrene	420	240	140	200	14	120	47	19	28	6.3
Anthracene	130	47	24	40	21	52	18	3.3	10	2.9
Fluoranthene	220	120	68	120	15	170	94	33	73	17
Pyrene	160	73	26	61	n.d.	140	68	11	44	n.d.
Benz[ <i>a</i> ]anthracene	110	32	15	20	3.6	150	55	10	22	1.7
Chrysene	81	34	25	31	6	150	57	33	45	15
Benzo[ <i>b</i> ]fluoranthene	120	37	39	38	23	200	81	53	75	42
Benzo[ <i>k</i> ]fluoranthene	34	13	9.5	12	5.3	97	27	15	25	9.0
Benz[ <i>a</i> ]pyrene	77	22	6.4	18	5.0	150	31	2.3	15	0.9
Indeno[ <i>cd</i> ]pyrene	61	14	17	14	14	150	39	23	33	20
Dibenz[ <i>a,h</i> ]anthracene	19	4.5	4.9	4.2	3.0	52	10	7.6	n.d.	5.3
Benzo[ <i>ghi</i> ]perylene	47	12	13	12	11	120	32	17	28	15
Sum of PAHs	2218	762	449	666	170	1759	604	235	427	139
PAH decrease (%)		66	80	70	92		66	87	76	92
LMW/HMW <sup>a</sup>	3.1	3.5	2.4	3.5	1.4	0.6	0.8	0.5	0.8	0.3
9-Fluorenone	300	270	280	250	170	48	34	22	18	14
Anthracene-9,10-dione	72	50	60	45	40	33	17	11	11	7.9
Benzo[ <i>de</i> ]anthracene- 7-one	3.2	5.0	n.d.	5.0	n.d.	39	6.5	4.2	4.9	n.d.
Benzo[ <i>a</i> ]anthracene- 7,12-dione	n.d.	5.5	22	5.9	11	20	6.3	19	5.8	18
Sum of O-PACs	375	331	362	306	221	140	64	56	40	40
O-PAC decrease (%)		12	3	18	41		54	60	71	71
%O-PAC (/total PAC)	14	30	45	31	57	7	10	19	9	22

253 <sup>a</sup>LMW/HMW = ratio of sum of naphthalene to pyrene relative to sum of benzo[*a*]anthracene to benzo[*ghi*]perylene

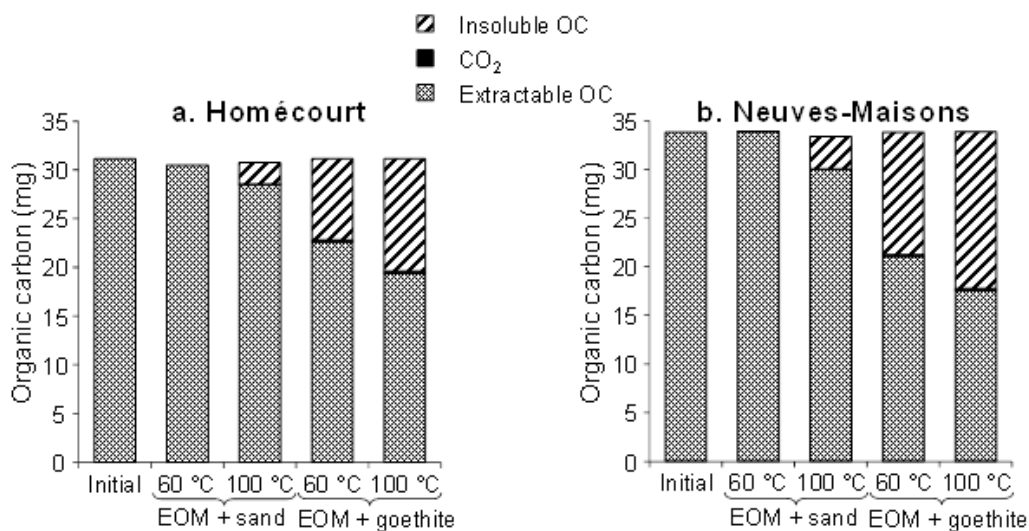
254 **4. Discussion**

255

256 4.1. Mechanisms of goethite-activated EOM oxidation

257 Overall, goethite showed a high reactivity during the EOM oxidation as CO<sub>2</sub> production and  
258 the PAH degradation rate were enhanced by its presence. However, it should be noted that the  
259 mineralization was of less importance because the amount of produced CO<sub>2</sub> during the  
260 experiment remained very low (< 7% of TOC).

261 To give a better insight into the main process involved in the reduction of the PAH and EOM  
262 contents, a carbon mass balance was performed (Figure 3). It showed that most of the carbon  
263 from the initial EOM was transferred to the insoluble compartment. Such observations were  
264 made in previous studies (Ghislain et al., 2010; Biache et al., 2011; Biache et al., 2014) where  
265 air-oxidation of PAH associated with active minerals led to the decrease in EOM content and  
266 to the formation of an insoluble carbonaceous residue resulting from oxidation-induced  
267 polymerization.



268

269 *Figure 3: Carbon mass balance of the initial and oxidized samples of extractable organic matters*  
270 *(EOMs) mixed with mineral phases (OC: organic carbon).*

271 EOM oxidations also induced an O-PAC production (ketones). Such compounds are known to  
272 be produced during PAH oxidation in various contexts i.e. chemical oxidation (Lundstedt et  
273 al., 2006), photo-degradation (Barbas et al., 1996) and biodegradation (Kazunga and Aitken,  
274 2000). As the O-PAC production was much more important in the EOM/goethite mixture than  
275 in the EOM/sand mixture, goethite seems to play an active part in the oxidation process. The  
276 oxidation of organic compounds on goethite is known to be initiated by the sorption and then  
277 formation of inner-sphere surface complexes with  $\text{Fe}^{\text{III}}$  surface sites (Pizzigallo et al., 1998).  
278 This chemical coordination at the goethite surface is a prerequisite for the electron transfer  
279 process (Stone and Morgan, 1987). Indeed, the sorbed molecule transfers an electron to  $\text{Fe}^{\text{III}}$   
280 site at goethite surfaces, leading to the formation of a very reactive cation radical that in turn  
281 interacts with oxygen to produce oxygenated species (McBride, 1987). Finally, dissociation of  
282 surface complexes and release of oxygenated species may occur, while the newly generated  
283  $\text{Fe}^{\text{II}}$  may be rapidly oxidized by  $\text{O}_2$ . Such mechanism was suggested for room temperature  
284 oxidation of organic compounds by  $\text{Mn}^{\text{VI}}$ - $\text{Mn}^{\text{III}}$ -oxides and  $\text{Fe}^{\text{III}}$ -oxides (McBride, 1987;  
285 Stone and Morgan, 1987).

286 Our observations, i.e. important decrease in PAH contents and important production of O-  
287 PACs, were consistent with the previously mentioned mechanism. This oxidation mechanism  
288 must be favored by the increasing temperature, since more decay in EOM and PAH contents  
289 and more O-PAC production were noted at 100 than at 60°C. Generally, the electron transfer  
290 process induced by chemical complexation is considered as endothermic and therefore  
291 improved by increasing temperature (Chidsey, 1991).

292 Moreover, several studies dealing with the  $\text{Fe}^{\text{III}}$ - or  $\text{Mn}^{\text{III/IV}}$ -induced oxidation of aromatic  
293 compounds have pointed out same polymerization/condensation process as observed in this  
294 study (Li et al., 2003; Arroyo et al., 2005; Russo et al., 2005).

295

296 4.2. Impact of goethite addition on the soil contamination.

297 When comparing the PAH decrease rates of both experiments (EOMs and soils), whole soils  
298 seemed to be more reactive. Goethite addition had a different impact on the whole soil vs the  
299 isolated EOM. While more decay in PAH concentration was observed in the presence of  
300 goethite, less CO<sub>2</sub> was produced and O-PAC concentrations decreased. The EOM content did  
301 not change significantly compared to the soil without goethite. The first explanation for these  
302 differences is the presence in the soils of other –mineral and organic– reactive surfaces.  
303 Previous studies dealing with biotic and abiotic oxidation of PAH contaminated matrices have  
304 already pointed out a high reactivity of complex soil systems (Biache et al., 2011; Biache et  
305 al., 2013; Biache et al., 2014) which has been attributed to the presence of reactive phases  
306 such as clay minerals, metal oxides and organic macromolecules. Both soils contain such  
307 reactive minerals (Biache et al., 2014), which may explain why the decrease in PAH and  
308 EOM contents were already high in the soil without goethite addition. Similar mechanisms of  
309 PAH oxidation could be involved here as in the EOM experiment but other by-products may  
310 be formed. The decrease in O-PAC contents may be explained by a strong  
311 sorption/sequestration in the soil and/or incorporation in the macromolecular network via  
312 polymerization. The high decay of EOM in the whole soil compared to the EOM/mineral  
313 mixture tends to support this hypothesis.

314 The goethite major impact was to reduce the CO<sub>2</sub> production in the whole soil experiment  
315 even if the CO<sub>2</sub> amount remained very low in all investigated experiments (less than 7‰ and  
316 4‰ of the Homécourt and Neuves-Maisons soils, respectively). This slight discrepancy “soil  
317 vs soil/goethite” might be due to CO<sub>2</sub> adsorption on goethite surfaces, but this process cannot  
318 be quantitatively evaluated in soil complex systems (Russell et al., 1975).

319

#### 320 4.3. Impact of initial soil composition on the OM reactivity

321 While both EOMs exhibited similar global trends during oxidations, some molecular-level  
322 differences can be observed. For example during the mineral/EOM oxidation, O-PAC  
323 compounds were produced for both EOMs; however the distribution of the generated  
324 compounds was different (Table 1, Figures S5 and S6). Indeed, the main O-PACs produced  
325 during Homécourt EOM oxidation were 3-ring O-PACs (9-fluorenone and anthracene-9,10-  
326 dione) whereas for Neuves-Maisons EOM oxidation, 4-ring O-PACs (benzo[*de*]anthracene-7-  
327 one and benz[*a*]anthracene-7,12-dione) were predominantly generated. These discrepancies  
328 can be attributed to differences in the initial PAH soil composition; Homécourt sample being  
329 dominated by 3-ring PAHs (Table 1, Figure S3) and Neuves-Maisons being dominated by 4-  
330 and 5-ring PAHs (Table 1, Figure S4). It is worthwhile noting that PAHs are known to be  
331 precursors of O-PAC formation. For instance 9-fluorenone is known to be one of the  
332 oxidation product of fluorene (Lee et al., 2001) which occurs in high concentration in  
333 Homécourt sample and, similarly, benz[*a*]anthracene-7,12-dione can be generated during  
334 benz[*a*]anthracene oxidation (Lee et al., 2001) which is one of the major PAHs of Neuves-  
335 Maisons sample.

336 Difference of the initial sample composition also seems to influence the sample response to  
337 oxidation. For both EOM/mineral and soil oxidations, the decrease in EOM contents was  
338 more important for Neuves-Maisons samples than for Homécourt (Figure 2). As discussed,  
339 this decrease was a transfer of the organic carbon from the EOM to the insoluble fraction  
340 which was more important for Neuves-Maisons than for Homécourt (Figure 3). The latter  
341 observation can be due to the fact that Neuves-Maisons sample presented higher proportion of

342 HMW compounds than Homécourt and HMW compounds are more inclined to be stabilized  
343 (condensed) in the non-extractable fraction (Northcott and Jones, 2001).

344

## 345 **5. Summary and conclusion**

346 In all experiments, oxidation led to (i) a decrease in PAH concentrations, (ii) a low production  
347 of CO<sub>2</sub> and (iii) a decrease in EOM content due to a condensation/polymerization  
348 phenomenon evidenced by a carbon mass balance. Oxidation of the EOM/minerals also led to  
349 a production of O-PACs, the initial PAH soil composition governing the type of generated  
350 compounds. The oxidation effects were more pronounced for EOM/goethite mixture than for  
351 EOM/silica sand mixture. These observations are consistent with the famous goethite-induced  
352 transformation mechanism of organic compounds. After PAC sorption on goethite surfaces,  
353 electron transfer process occurs leading to the formation of reactive cation radical that in turn  
354 interacts with oxygen or oxygen-species yielding oxidized products.

355 As in EOM experiments, goethite addition to the whole soils affected OM oxidation, but in a  
356 lesser extent. This limited effect was likely due to the presence of a significant amount of  
357 reactive phases naturally occurring in the soils. The soil initial composition also impacted its  
358 evolution during oxidation; higher abundance of HMW compounds favoring the formation of  
359 an insoluble residue and therefore EOM stabilization.

360 These conclusions showed that goethite may play a part in natural attenuation of PAH  
361 contaminated soils as it contributes to contamination stabilization during low-temperature air-  
362 oxidation. This work provides first results of the mechanisms involved and also underlined  
363 the potential of indigenous reactive minerals to stabilize organic contamination. Therefore  
364 their impact on the fate and transformation of PAHs in soils under different conditions  
365 (humidity, temperature, oxygen concentrations) more representative of the field should be

366 investigated , and the long-term behavior of the refractory compounds generated during  
367 oxidation (e.g. insoluble carbonaceous residues) should be explored.

368

### 369 **Acknowledgements**

370 We thank the GISFI (French Scientific Interest Group - Industrial Wasteland  
371 (<http://www.gisfi.prd.fr>). We thank Pr. Christian Ruby from the LCPME laboratory (Nancy)  
372 for supplying us with the goethite.

373

### 374 **References**

- 375 Arroyo, L.J., Li, H., Teppen, B.J., Johnston, C.T., Boyd, S.A., 2005. Oxidation of 1-naphthol  
376 coupled to reduction of structural Fe<sup>3+</sup> in smectite. *Clays Clay Miner.* 53, 587-596.
- 377 Barbas, J.T., Sigman, M.E., Dabestani, R., 1996. Photochemical oxidation of phenanthrene  
378 sorbed on silica gel. *Environ. Sci. Technol.* 30, 1776-1780.
- 379 Biache, C., Faure, P., Mansuy-Huault, L., Cébron, A., Beguiristain, T., Leyval, C., 2013.  
380 Biodegradation of the organic matter in a coking plant soil and its main constituents.  
381 *Org. Geochem.* 56, 10-18.
- 382 Biache, C., Ghislain, T., Faure, P., Mansuy-Huault, L., 2011. Low temperature oxidation of a  
383 coking plant soil organic matter and its major constituents: An experimental approach to  
384 simulate a long term evolution. *J. Hazard. Mater.* 188, 221-230.
- 385 Biache, C., Kouadio, O., Lorgeoux, C., Faure, P., 2014. Impact of clay mineral on air  
386 oxidation of PAH-contaminated soils. *Environ Sci Pollut Res*, 1-10.
- 387 Blanchart, P., Faure, P., Bruggeman, C., De Craen, M., Michels, R., 2012. In situ and  
388 laboratory investigation of the alteration of Boom Clay (Oligocene) at the air–

389 geological barrier interface within the Mol underground facility (Belgium):  
390 Consequences on kerogen and bitumen compositions. *Appl. Geochem.* 27, 2476-2485.

391 Borch, T., Kretzschmar, R., Kappler, A., Cappellen, P.V., Ginder-Vogel, M., Voegelin, A.,  
392 Campbell, K., 2009. Biogeochemical redox processes and their impact on contaminant  
393 dynamics. *Environ. Sci. Technol.* 44, 15-23.

394 Calemma, V., Rausa, R., Margarit, R., Girardi, E., 1988. FT-i.r. study of coal oxidation at low  
395 temperature. *Fuel* 67, 764-770.

396 Chidsey, C.E.D., 1991. Free energy and temperature dependence of electron transfer at the  
397 metal-electrolyte Interface. *Science* 251, 919-922.

398 Elie, M., Faure, P., Michels, R., Landais, P., Griffault, L., 2000. Natural and laboratory  
399 oxidation of low-organic-carbon-content sediments: comparison of chemical changes in  
400 hydrocarbons. *Energy Fuels* 14, 854-861.

401 Faure, P., Landais, P., Griffault, L., 1999. Behavior of organic matter from Callovian shales  
402 during low-temperature air oxidation. *Fuel* 78, 1515-1525.

403 Gethner, J.S., 1987. Kinetic study of the oxidation of Illinois No. 6 coal at low temperatures:  
404 Evidence for simultaneous reactions. *Fuel* 66, 1091-1096.

405 Ghislain, T., Faure, P., Biache, C., Michels, R., 2010. Low-temperature, mineral-catalyzed air  
406 oxidation: a possible new pathway for PAH stabilization in sediments and soils.  
407 *Environ. Sci. Technol.* 44, 8547-8552.

408 Jakab, E., Hoesterey, B., Windig, W., Hill, G.R., Meuzelaar, H.L.C., 1988. Effects of low  
409 temperature air oxidation (weathering) reactions on the pyrolysis mass spectra of US  
410 coals. *Fuel* 67, 73-79.

411 Kazunga, C., Aitken, M.D., 2000. Products from the incomplete metabolism of pyrene by  
412 polycyclic aromatic hydrocarbon-degrading bacteria. *Appl. Environ. Microbiol.* 66,  
413 1917-1922.

414 Lee, B.-D., Iso, M., Hosomi, M., 2001. Prediction of Fenton oxidation positions in polycyclic  
415 aromatic hydrocarbons by Frontier electron density. *Chemosphere* 42, 431-435.

416 Li, H., Lee, L.S., Schulze, D.G., Guest, C.A., 2003. Role of soil manganese in the oxidation  
417 of aromatic amines. *Environ. Sci. Technol.* 37, 2686-2693.

418 Lin, K., Ding, J., Wang, H., Huang, X., Gan, J., 2012. Goethite-mediated transformation of  
419 bisphenol A. *Chemosphere* 89, 789-795.

420 Lundstedt, S., Persson, Y., Öberg, L., 2006. Transformation of PAHs during ethanol-Fenton  
421 treatment of an aged gasworks' soil. *Chemosphere* 65, 1288-1294.

422 McBride, M.B., 1987. Adsorption and oxidation of phenolic compounds by iron and  
423 manganese oxides. *Soil Sci. Soc. Am. J.* 51, 1466-1472.

424 Nam, K., Rodriguez, W., Kukor, J.J., 2001. Enhanced degradation of polycyclic aromatic  
425 hydrocarbons by biodegradation combined with a modified Fenton reaction.  
426 *Chemosphere* 45, 11-20.

427 Northcott, G.L., Jones, K.C., 2001. Partitioning, extractability, and formation of  
428 nonextractable PAH residues in soil. 1. Compound Differences in Aging and  
429 Sequestration. *Environ. Sci. Technol.* 35, 1103-1110.

430 Pizzigallo, M.D.R., Ruggiero, P., Crecchio, C., Mascolo, G., 1998. Oxidation of  
431 chloroanilines at metal oxide surfaces. *J. Agr. Food Chem.* 46, 2049-2054.

432 Prélot, B., Villiéras, F., Pelletier, M., Gérard, G., Gaboriaud, F., Ehrhardt, J.-J., Perrone, J.,  
433 Fedoroff, M., Jeanjean, J., Lefèvre, G., Mazerolles, L., Pastol, J.-L., Rouchaud, J.-C.,  
434 Lindecker, C., 2003. Morphology and surface heterogeneities in synthetic goethites. *J.*  
435 *Colloid Interface Sci.* 261, 244-254.

436 Russell, J.D., Paterson, E., Fraser, A.R., Farmer, V.C., 1975. Adsorption of carbon dioxide on  
437 goethite ( $\alpha$ -FeOOH) surfaces, and its implications for anion adsorption. *J. Chem. Soc.,*  
438 *Faraday Trans.* 71, 1623-1630.

439 Russo, F., Rao, M., Gianfreda, L., 2005. Bioavailability of phenanthrene in the presence of  
440 birnessite-mediated catechol polymers. *Appl. Microbiol. Biotechnol.* 68, 131-139.

441 Schwertmann, U., Cornell, R.M., 2007. Goethite. in *Iron oxides in the laboratory* 2<sup>nd</sup> Ed.  
442 Wiley-VCH Verlag GmbH, pp. 67-92.

443 Schwertmann, U., Taylor, R.M., 1989. Iron Oxides. in: Dixon, J.B., Weed, S.B. (Eds.).  
444 Minerals in soil environments. Soil Science Society of America, pp. 379-438.

445 Stone, A.T., Morgan, J.J., 1987. Reductive dissolution of metal oxides. in: *Aquatic surface*  
446 *chemistry: chemical processes at the particle-water interface.* John Wiley and Sons,  
447 New York. 1987. p 221-254.

448 Sumner, M.E. (Ed.), 2000. *Handbook of soil science.* CRC Press LLC.

449 Usman, M., Faure, P., Lorgeoux, C., Ruby, C., Hanna, K., 2013. Treatment of hydrocarbon  
450 contamination under flow through conditions by using magnetite catalyzed chemical  
451 oxidation. *Environ Sci Pollut Res* 20, 22-30.

452 Usman, M., Faure, P., Ruby, C., Hanna, K., 2012. Remediation of PAH-contaminated soils by  
453 magnetite catalyzed Fenton-like oxidation. *Appl. Catal., B* 117–118, 10-17.

454 Wang, Y., Liu, C.S., Li, F.B., Liu, C.P., Liang, J.B., 2009. Photodegradation of polycyclic  
455 aromatic hydrocarbon pyrene by iron oxide in solid phase. *J. Hazard. Mater.* 162, 716-  
456 723.

457 Watts, R.J., Stanton, P.C., 1999. Mineralization of sorbed and NAPL-phase hexadecane by  
458 catalyzed hydrogen peroxide. *Water Res.* 33, 1405-1414.

459 Yap, C.L., Gan, S., Ng, H.K., 2011. Fenton based remediation of polycyclic aromatic  
460 hydrocarbons-contaminated soils. *Chemosphere* 83, 1414-1430.

461 Zhang, H., Huang, C.-H., 2007. Adsorption and oxidation of fluoroquinolone antibacterial  
462 agents and structurally related amines with goethite. *Chemosphere* 66, 1502-1512.